

**A hollow cage-like layered double hydroxide modified carbon paste electrode as an efficient catalyst for electrochemical water oxidation in neutral media**

Li Yu,\* Xiaocai Ma, Qin Liang, Yuqing Fan

*College of Chemistry and Chemical Engineering, Xinyang Normal University,*

*Xinyang 464000, China.*

\* To whom correspondence should be addressed.

E-mail addresses: [yulisunshine@163.com](mailto:yulisunshine@163.com)

**Materials.** All chemicals were purchased from Aladdin (analytical grade) and used without any further purification. The aqueous solutions were prepared using doubledistilled deionized water (Milli-Q grade, Millipore).

**Physical Methods.** Brunauer–Emmett–Teller (BET) surface area was determined using N<sub>2</sub> adsorption/desorption isotherm measurements at -196 °C on a Micrometrics TriStar 3000 equipment. Powder X-ray diffraction (PXRD) results were obtained with a PANalyticalX'Pert Pro Diffractometer handled at 40 kV and 40 mA with Cu K $\alpha$  radiation in the 2 $\theta$  range of 10°-90°. X-Ray photoelectron spectra (XPS) were measured by ESCALAB250xi with X-ray monochromatisation. Infrared spectra (2–4 wt% sample in KBr pellets) were recorded using a Bruker VERTEX 70v FT-IR spectrometer. Transmission electron microscopy (TEM) and high-resolution TEM (HRTEM) images were carried out on JEOL-2100F apparatus at an accelerating voltage of 200 kV. Elemental mapping and energy dispersive X-ray spectroscopy (EDS) were performed with JSM-5160LV-Vantage typed energy spectrometer.

**Electrochemical Measurements.** The electrocatalytic water oxidation abilities of LDHs-based electrode materials were tested in 0.2 M Tris-HCl buffer solution (pH=7.1) using a CHI660D electrochemical analyzer at room temperature (scan rate: 60 mV/s). For a standard three-electrode configuration, an amorphous carbon paste (0.07 cm<sup>2</sup>), Ag/AgCl (KCl 3 M), and platinum wire electrodes were employed as working, reference, and counter electrodes, respectively.

The electrochemical measurements of catalysts were carried out by linear scan voltammogram (LSV) and cyclic voltammetry (CV) at a potential range of 0.6–1.8 V (vs. RHE) and a rate of 60 mV/s. Chronoamperometry was used to investigate the stability of the electrode, and chronoamperometry tests were implemented at a constant overpotential of 120 mV, and this constant voltage was applied for 30 min before the measurements for signal stabilization. In order to further explore the

recovery catalysts, FTO is regarded as a working electrode to replace the carbon paste electrode. The catalyst powder was grinded and deposited on FTO electrode via a drop-casting method. After the simulative test of water electrolysis at a constant overpotential of 120 mV in Tris-HCl buffer solution, the as-used Ni<sub>1</sub>Co<sub>4</sub>-LDH electrode was taken out from the buffer solution and washed with anhydrous ethanol, followed by drying in the air for further characterizations. After the recovered electrode material was carefully scraped off from the FTO and washed with anhydrous ethanol for three times, collected and then dried at room temperature, we then carried out TEM and XPS to analyze the stability of the recovered powder [1]. Electrochemical impedance spectroscopy (EIS) analysis of electrode material was implemented using above three electrode systems. The frequency range was 100 000 Hz to 0.1 Hz, and the amplitude of the applied voltage was 5 mV.

The electrode material was fabricated as follows: 870/770/500 mg graphite powder was added to the solution of 2 mL acetone containing 130/230/500 mg Ni<sub>x</sub>Co<sub>y</sub>-LDHs and the mixture was ultrasonically mixed for 3 min, followed by evaporation of acetone, which produced rather homogeneously covered graphite particles. To the graphite particles 0.66 mL Nujol was added and stirred with a glass stick. The homogenized mixture was used to pack 3 mm inner diameter glass tubes to a length of 0.8 cm from one of their ends. In addition, a little extra mixture was retained on the top of the electrodes, and the mixture in the tubes was pressed lightly on smooth plastic paper with a copper stick through the back. The electrical contact was established with the copper stick. The bare carbon paste electrode was fabricated using the same procedure as described above except that the modifier in acetone was not added. The surface of the carbon paste electrode was wiped with weighing paper.

**Synthesis of Ni<sub>x</sub>Co<sub>y</sub>-LDHs.** Ni<sub>x</sub>Co<sub>y</sub>-LDHs were prepared according to the literature [2] with some amendment. First, a solution of 2.49 g of Co(NO<sub>3</sub>)<sub>2</sub>·6H<sub>2</sub>O in

250 mL of methyl alcohol was added to 250 mL of an aqueous solution containing 3.28 g of 2-methylimidazole with methyl alcohol. The as-synthesized purple solution was sedimented for 24 h and centrifuged. After washing with methyl alcohol for several times and then dried at 45 °C for 24 h, ZIF-67 was collected. Second, for preparation of  $\text{Ni}_x\text{Co}_y\text{-LDHs}$ , different mass ratios of Ni/Co system (4:1, 1:1, 1:4, 1:6 and 1:8 for the synthesis of  $\text{Ni}_4\text{Co}_1\text{-LDH}$ ,  $\text{Ni}_1\text{Co}_1\text{-LDH}$ ,  $\text{Ni}_1\text{Co}_4\text{-LDH}$ ,  $\text{Ni}_1\text{Co}_6\text{-LDH}$  and  $\text{Ni}_1\text{Co}_8\text{-LDH}$ , respectively) was collected by mixing  $\text{Ni}(\text{NO}_3)_2 \cdot 6\text{H}_2\text{O}$  and  $\text{Co}(\text{NO}_3)_2 \cdot 6\text{H}_2\text{O}$  in 50 ml ethanol include 60 mg ZIF-67, while the total amount of metal salts ( $\text{Ni}(\text{NO}_3)_2 \cdot 6\text{H}_2\text{O} + \text{Co}(\text{NO}_3)_2 \cdot 6\text{H}_2\text{O}$ ) was kept to 200 mg. The above mixture solution was refluxed for 1 h and allowed to cool slowly. These products were obtained by centrifugation, washed with ethanol for several times, and then dried at 45 °C for 24 h.

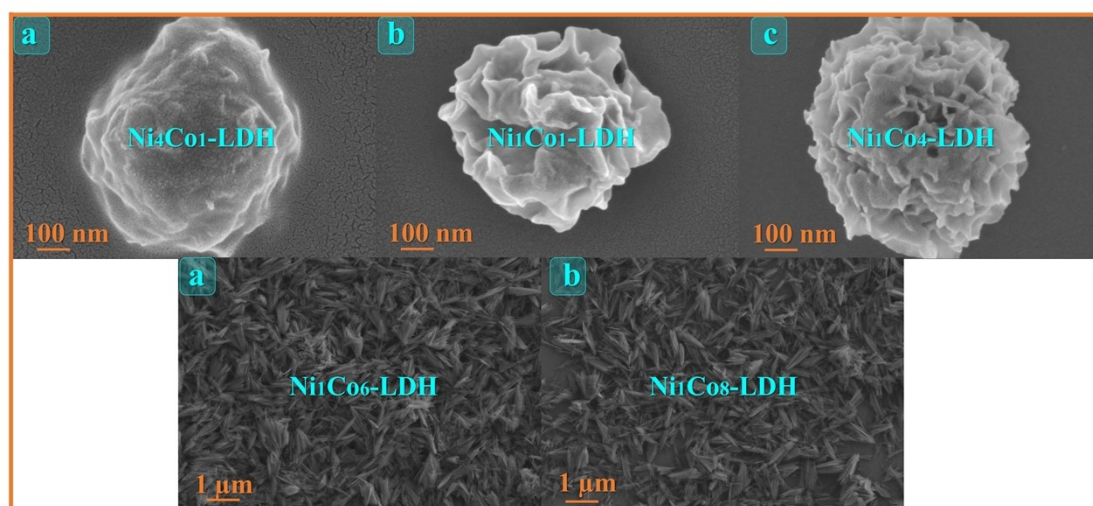


**Fig. S1** SEM images of  $\text{Ni}_4\text{Co}_1\text{-LDH}$ ,  $\text{Ni}_1\text{Co}_1\text{-LDH}$ ,  $\text{Ni}_1\text{Co}_4\text{-LDH}$ ,  $\text{Ni}_1\text{Co}_6\text{-LDH}$  and  $\text{Ni}_1\text{Co}_8\text{-LDH}$ .

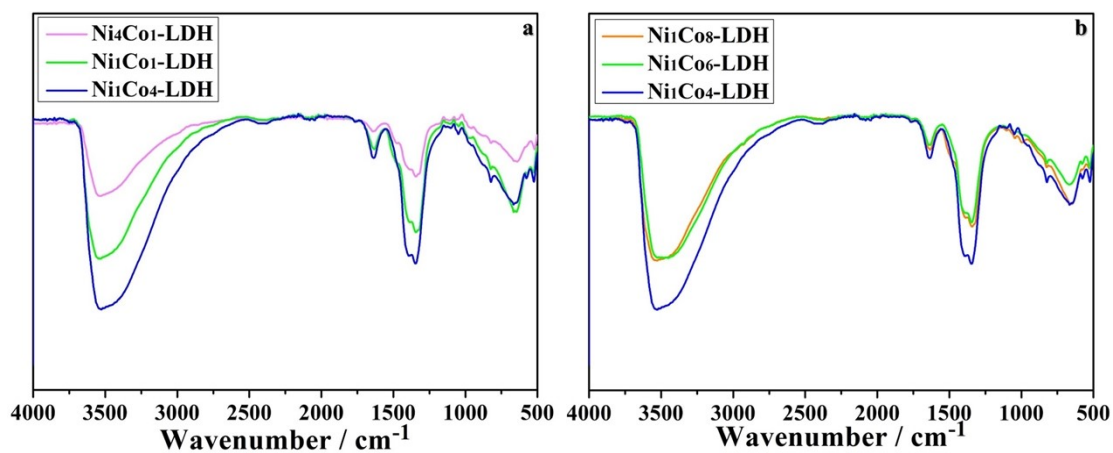


**Fig. S2** FT-IR spectra of Ni<sub>4</sub>Co<sub>1</sub>-LDH, Ni<sub>1</sub>Co<sub>1</sub>-LDH, Ni<sub>1</sub>Co<sub>4</sub>-LDH, Ni<sub>1</sub>Co<sub>6</sub>-LDH and Ni<sub>1</sub>Co<sub>8</sub>-LDH.

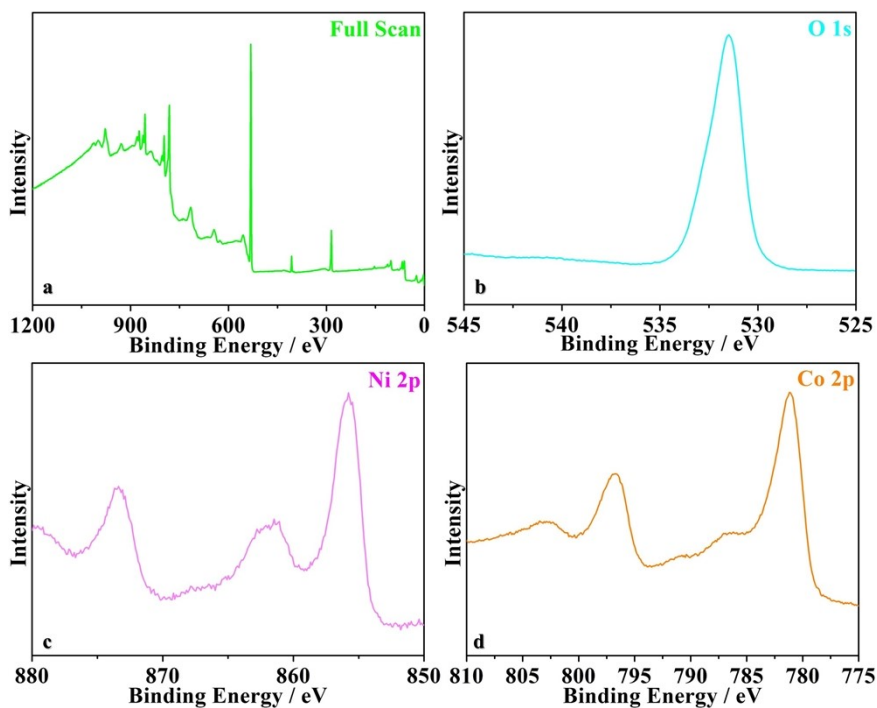


**Fig. S3** X-ray photoelectron spectra of Ni<sub>1</sub>Co<sub>4</sub>-LDH in the energy regions of (a) full scan, (b) O 1s, (c) Ni 2p, (d) Co 2p.

**Table S1** BET surface areas and structural parameters of samples

Catalyst	BET surfaces area (m <sup>2</sup> /g) <sup>a</sup>	Pore size (nm) <sup>b</sup>	Pore volume (cm <sup>3</sup> /g) <sup>c</sup>
Ni <sub>4</sub> Co <sub>1</sub> -LDH	21.9	1.6	0.1
Ni <sub>1</sub> Co <sub>1</sub> -LDH	41.1	2.8	0.3
Ni <sub>1</sub> Co <sub>4</sub> -LDH	58.3	2.2	0.3
Ni <sub>1</sub> Co <sub>6</sub> -LDH	9.8	17.2	0.02
Ni <sub>1</sub> Co <sub>8</sub> -LDH	12.2	15.5	0.02

<sup>a</sup> Surface area obtained from BET measurements.

<sup>b</sup> BJH desorption pore size distribution.

<sup>c</sup> BJH desorption pore volume.

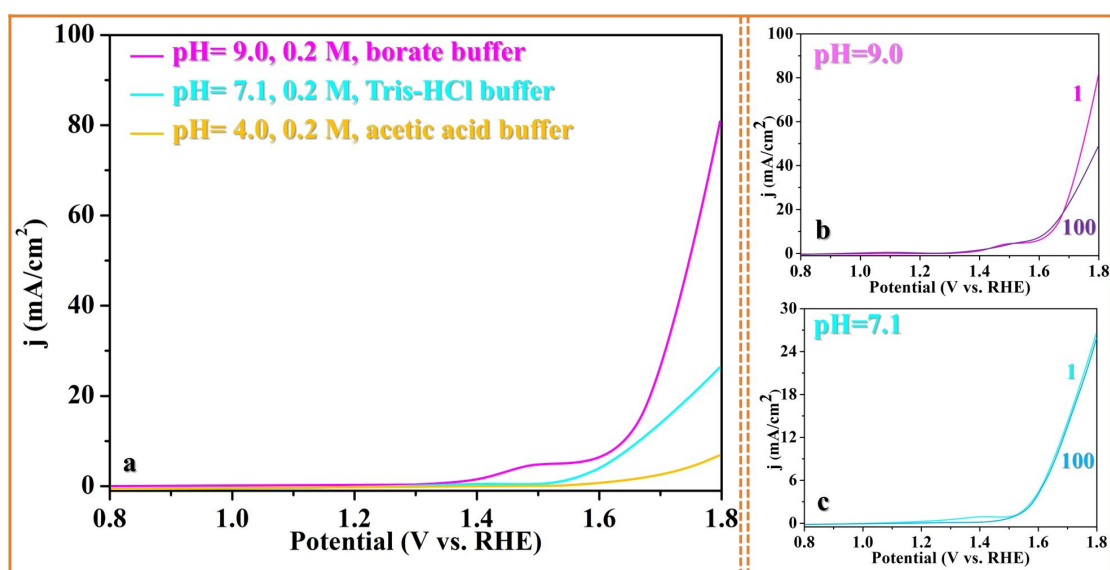


**Fig. S4** (a) Comparison of the LSV curves of Ni<sub>1</sub>Co<sub>4</sub>-LDH/C under three pH conditions. (b) LSV curves of Ni<sub>1</sub>Co<sub>4</sub>-LDH/C for 100 times of voltammetry cycling at pH 9.0. (c) LSV curves of Ni<sub>1</sub>Co<sub>4</sub>-LDHs/C for 100 times of voltammetry cycling at pH 7.1.

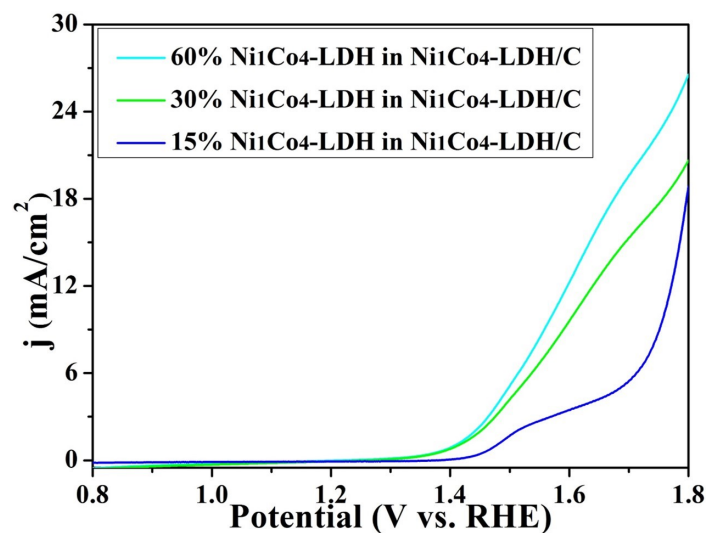


**Fig. S5 (a)** Comparison of the LSV curves of  $\text{Ni}_1\text{Co}_4\text{-LDH/C}$  with different  $\text{Ni}_1\text{Co}_4\text{-LDH}$  content in weight between 15 and 60% in 0.2 M Tris-HCl buffer solution (pH=7.1), scan rate: 60 mV/s.

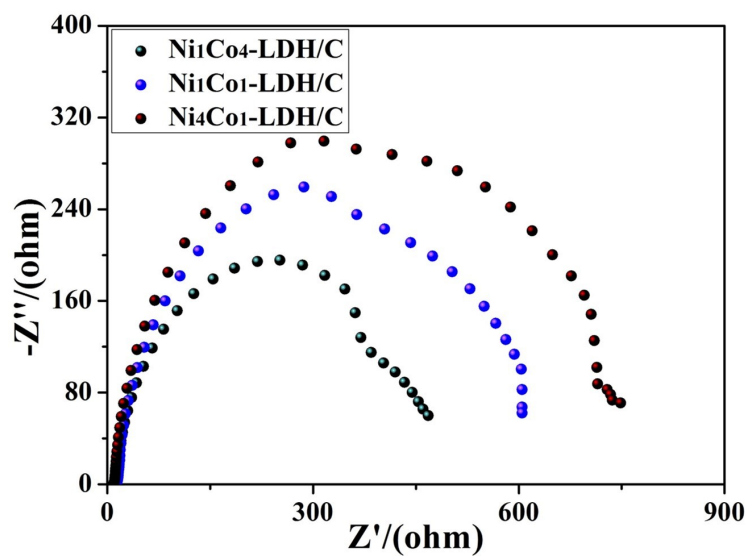


**Fig. S6** Nyquist plots of EIS for  $\text{Ni}_1\text{Co}_1\text{-LDH/C}$ ,  $\text{Ni}_1\text{Co}_4\text{-LDH/C}$ , and  $\text{Ni}_4\text{Co}_1\text{-LDH/C}$ .

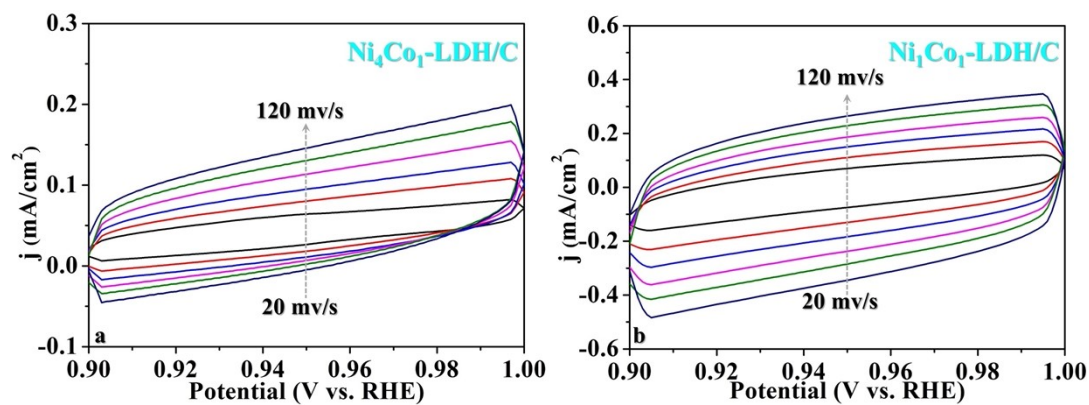


**Fig. S7** (a) CV curves measured within the range of 0.9 to 1.0 V vs. RHE with scan rate from 20 to 120 mV s<sup>-1</sup> of  $\text{Ni}_4\text{Co}_1\text{-LDH/C}$  (a) and  $\text{Ni}_1\text{Co}_1\text{-LDH/C}$  (b).

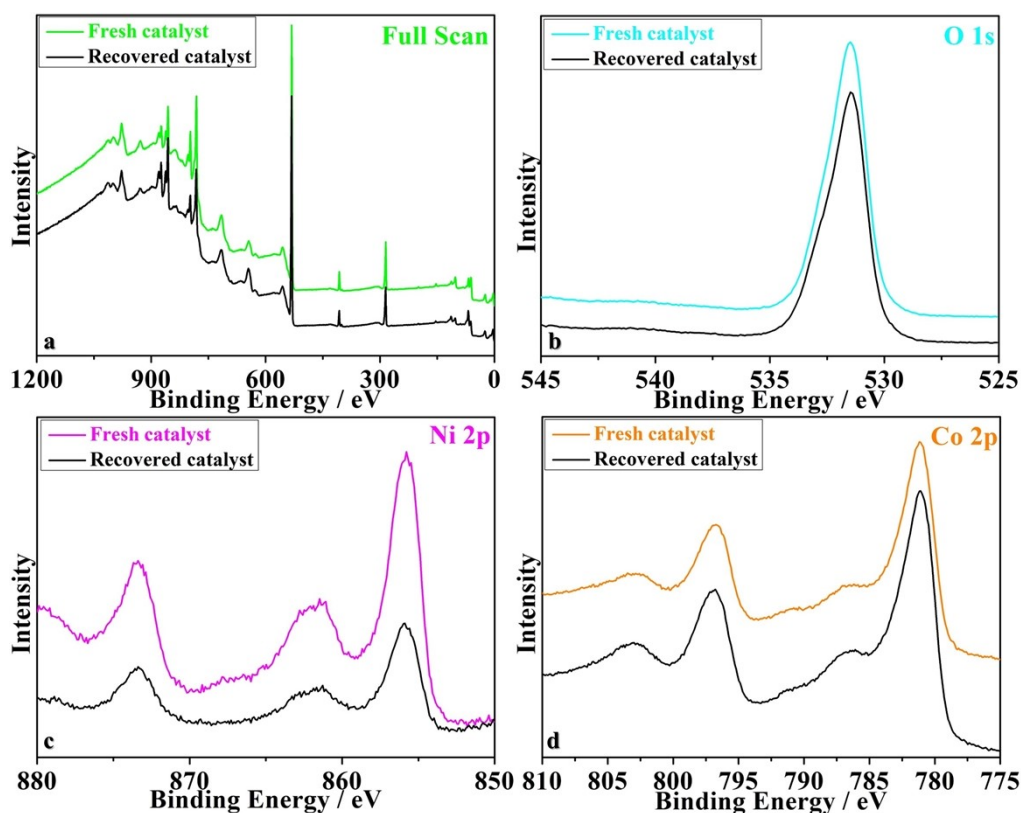


**Fig. S8** X-ray photoelectron spectra of  $\text{Ni}_1\text{Co}_4\text{-LDH}$  before and after the electrochemical stability experiment in the energy regions of (a) full scan, (b) O 1s, (c) Ni 2p, and (d) Co 2p.

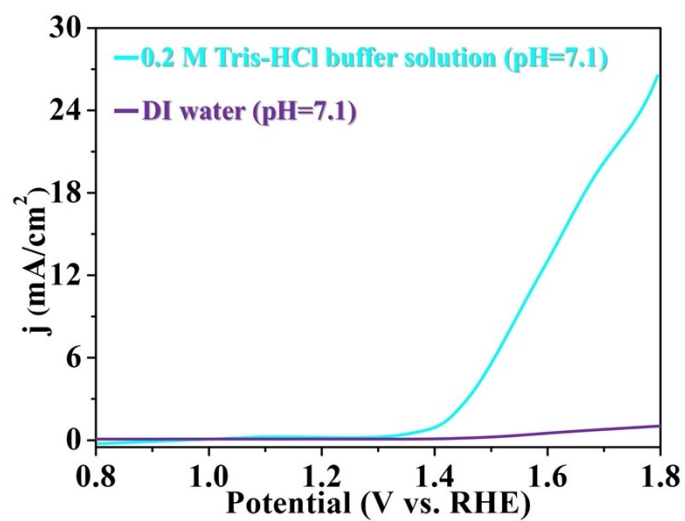


**Fig. S9** Comparison of the LSV curves of Ni<sub>1</sub>Co<sub>4</sub>-LDH/C under different reaction solution.

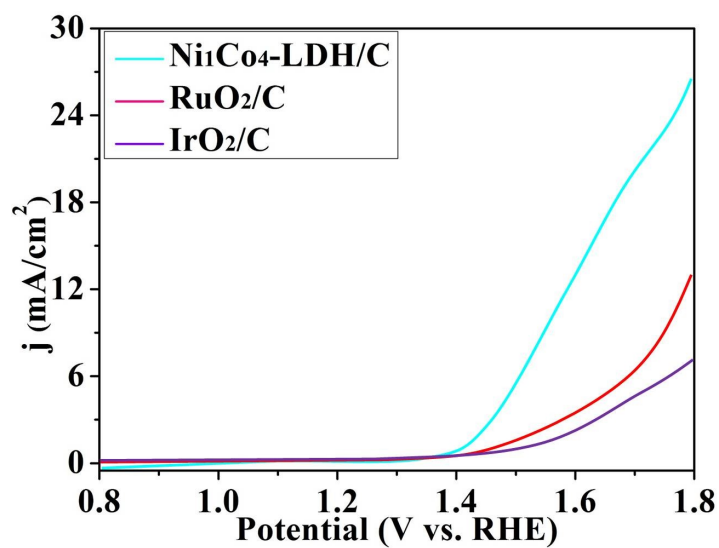


**Fig. S10** Comparison of the LSV curves of RuO<sub>2</sub>, IrO<sub>2</sub> and Ni<sub>1</sub>Co<sub>4</sub>-LDH in pH=7.1.

**Table S2** Water oxidation catalyzed by different catalysts

Entry	catalyst	$\eta/\text{mV}$ (10 mA/cm <sup>2</sup> )	Conditions	Ref.
1	chiral CuO@Ni	110	0.1 M KOH	Int. J. Hydrogen energy., 2021, 46, 8922.
2	Cu@NiFe-LDH	199	1.0 M KOH	Energy Environ. Sci., 2017, 10, 1820.
3	Co-RuO <sub>2</sub>	169	0.5 M H <sub>2</sub> SO <sub>4</sub>	iScience, 2020, 23, 100756.
4	Mn-RuO <sub>2</sub>	158	0.5 M H <sub>2</sub> SO <sub>4</sub>	ACS Catal., 2020, 10, 1152.
5	NiFe <sub>2</sub> O <sub>4</sub> /NiFeP	191	1.0 M KOH	ChemElectroChem, 2020, 7, 4047.
6	NiFe LDH- POM/NF	200	0.1 M KOH	Small, 2020, 2003777.
7	Mn <sub>3</sub> O <sub>4</sub>	395	0.5 M PBS, pH 7	Adv. Funct. Mater., 2020, 1910424.
8	Ni <sub>0.1</sub> Co <sub>0.9</sub> P	125	1 M PBS, pH 7	Angew. Chem. Int. Ed., 2018, 130, 15671.
9	Ni-doped Mn <sub>3</sub> O <sub>4</sub>	458	0.5 M PBS, pH 7	Small Methods, 2020, 1900733.
10	Ni-CoOOH/NF	410	1 M PBS, pH 7	Chem. Eng. J., 2020, 398, 125537.
11	Ni <sub>1</sub> Co <sub>4</sub> -LDH	120	0.2 M Tris-HCl pH 7.1	This work

## References

- [1] L. Yu, Q. Liang, X. Ma, X. Zuo. Efficient and stable Fe<sub>3</sub>O<sub>4</sub>@SiO<sub>2</sub> core-shell nanospheres for electrochemical water oxidation under neutral conditions. *New J. Chem.*, 2023, **47**, 4192–4196.
- [2] X. Zhang, W. Lu, Y. Tian, S. Yang, Q. Zhang, D. Lei and Y. Zhao. Nanosheet-assembled NiCo-LDH hollow spheres as high-performance electrodes for supercapacitors. *J. Colloid Interf. Sci.*, 2022, **606**, 1120–1127.